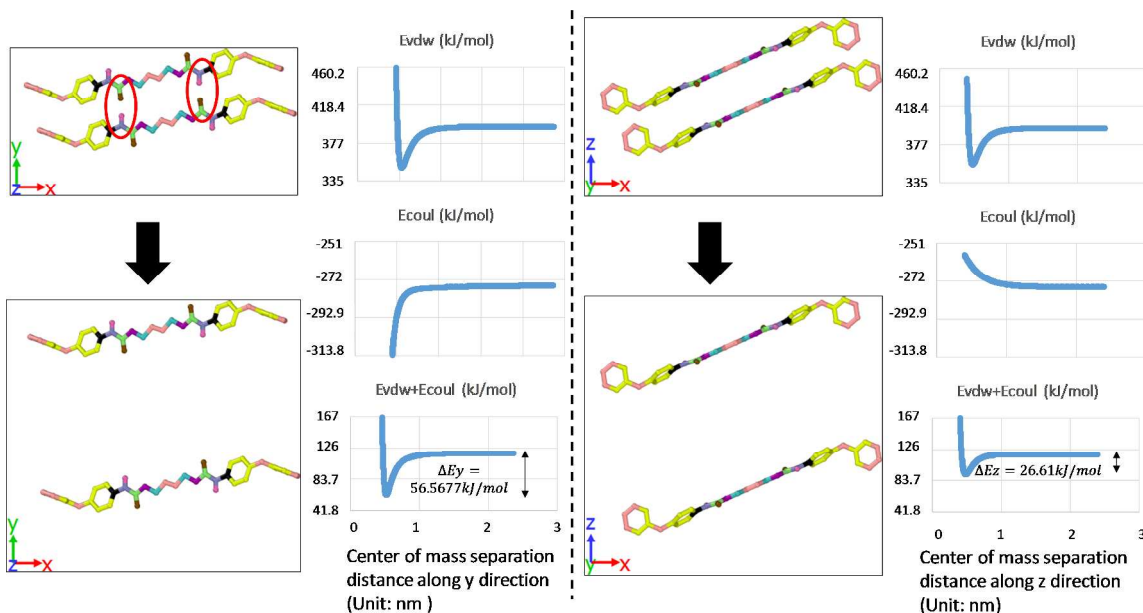


# Supporting Information

## Molecular Simulation of Thermoplastic Polyurethanes under Large Tensile Deformation

Shuze Zhu<sup>(1)</sup>, Nikolaos Lempesis<sup>(1)</sup>, Pieter J. in 't Veld<sup>(2)</sup>, Gregory. C. Rutledge<sup>(1)</sup>

- (1) Department of Chemical Engineering, Massachusetts Institute of Technology, Cambridge, MA 02139.  
 (2) BASF SE, ROM/AM, Carl Bosch Str, 38, 67056 Ludwigshafen, Germany



**Figure S1.** Estimation of hydrogen bonding strength represented by the force field in this work. Here, the interaction energy between two partial hard segments, stacked as they would be in the hard domain, are simulated with all atoms fixed. “Evdw” is the van der Waals energy output from LAMMPS, and “Ecoul” is the Coulombic energy output from LAMMPS. Left: separation in the y direction, directly breaking two hydrogen bonds (highlighted by red circles). Right: separation in the z direction, involving no breaking of hydrogen bonds. The nature of the Coulombic interaction energy is very different for the two directions, indicating that the Coulombic force resists separation in the y direction, but facilitates separation in the z direction. The hydrogen bonding energy was approximated by  $(\Delta E_y - \Delta E_z)/2 = 14.9787$  kJ/mol. The factor of 2 arises because there are two hydrogen bonds in the partial hard segments simulated.

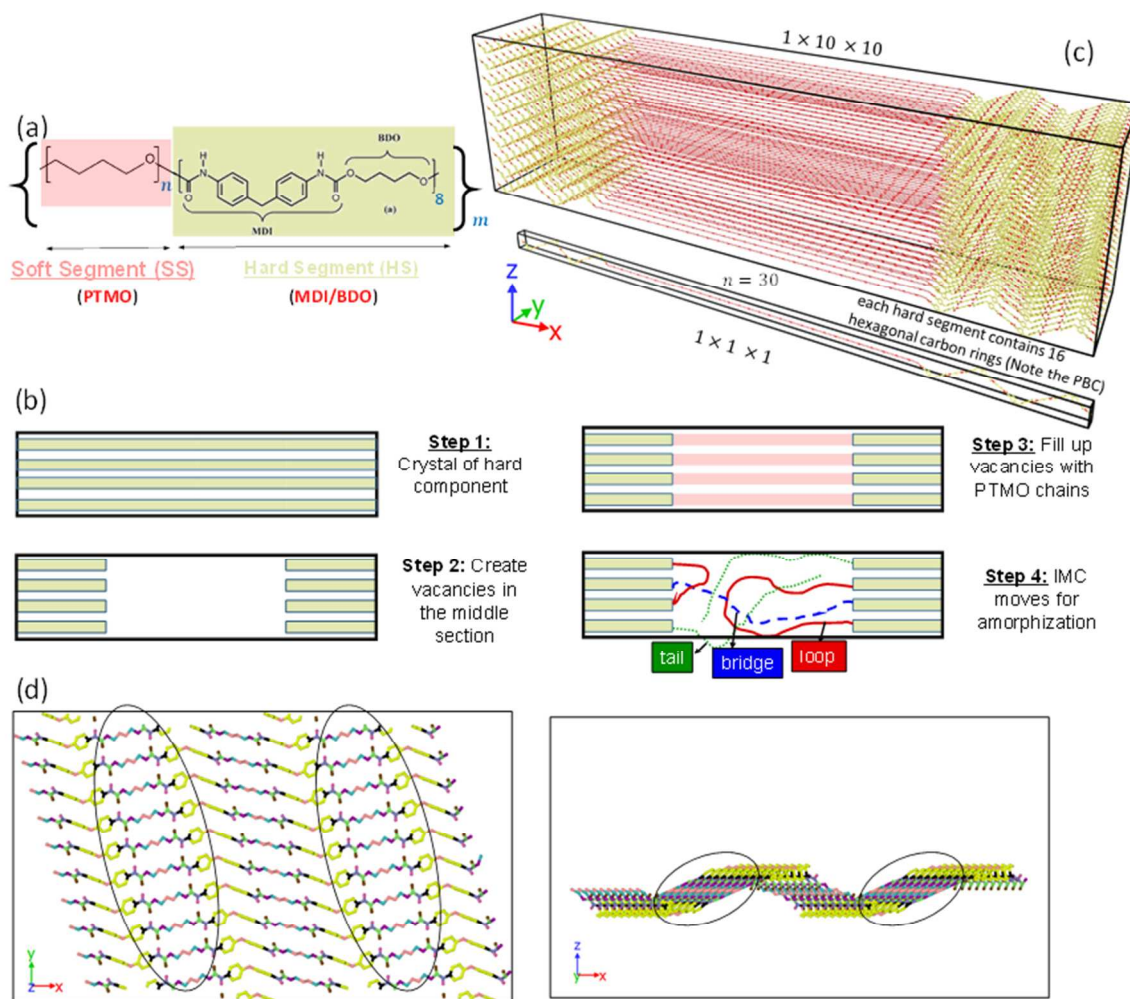


**Figure S2.** (a) Chemical multi-block structure of the TPU simulated in this work, where the MDI/BDO hard segment (HS) spans 4 unit cells (2 repeat units per unit cell) and the PTMO soft segment (SS) length is statistically distributed. As a result of the connectivity-altering moves and periodic boundary conditions, each simulation sampled from a distribution of multi-blocks of the form  $SS_t[-HS-SS_{l,b}]_m-HS-SS_t$ ,  $m=0,1,2,\dots$ , where the subscripts ' $t$ ' and ' $l,b$ ' denote either a tail block or a loop or bridge block, respectively. The types of SS blocks connected to a single HS block are essentially uncorrelated, resulting in a statistical distribution of multi-blocks, subject only to constraints imposed by the total number of tails, loops and bridges in the simulation. (b) Schematic showing the steps used to build the simulation model. The black box indicates the simulation cell with periodical boundary conditions. (c) Perspective view of the unit cell ( $1 \times 1 \times 1$ ) and supercell ( $1 \times 10 \times 10$ ) TPU united-atom models, before amorphization of the soft domain using IMC. Part (c) shows  $n=30$ , which corresponds to a mass fraction of hard component around 55%. (d) Illustration of hydrogen bonding plane in hard domain. The circled region denotes the rows of hydrogen bonds within hydrogen bonded planes.

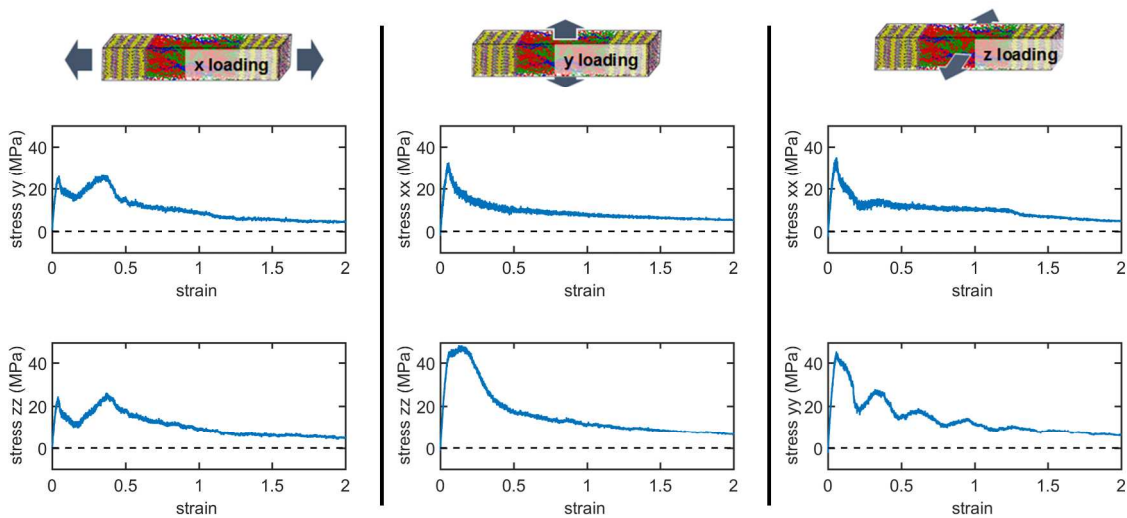


**Figure S3.** Engineering stress-strain curves showing the normal stress components orthogonal to the direction of tensile deformation, averaged over all configurations. Columns separated by solid lines denote the corresponding loading directions (x, y and z), which are orthogonal to each other. For each loading direction, there are two normal stress components that are orthogonal to the loading direction. The normal stress components along loading direction are reported in main text.

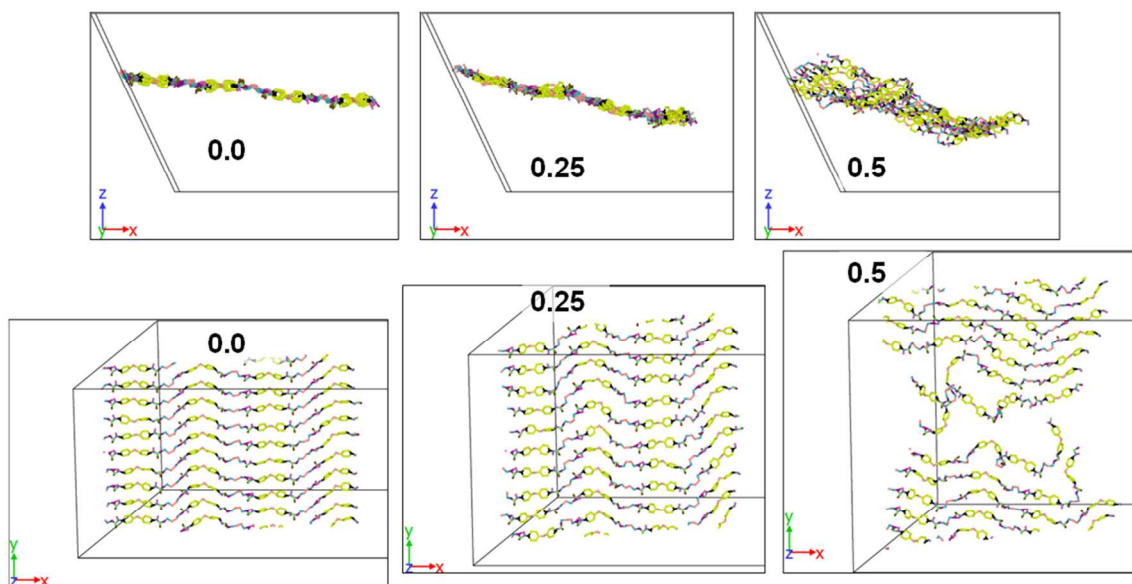


**Figure S4.** Evolution of structure for the hard domain of configuration #1 (“No bridges” topological sub-ensemble) under tensile deformation along the y direction. Images are labeled with strain values. Here, only a slice in the hard domain is shown, representing the hydrogen bonding plane.

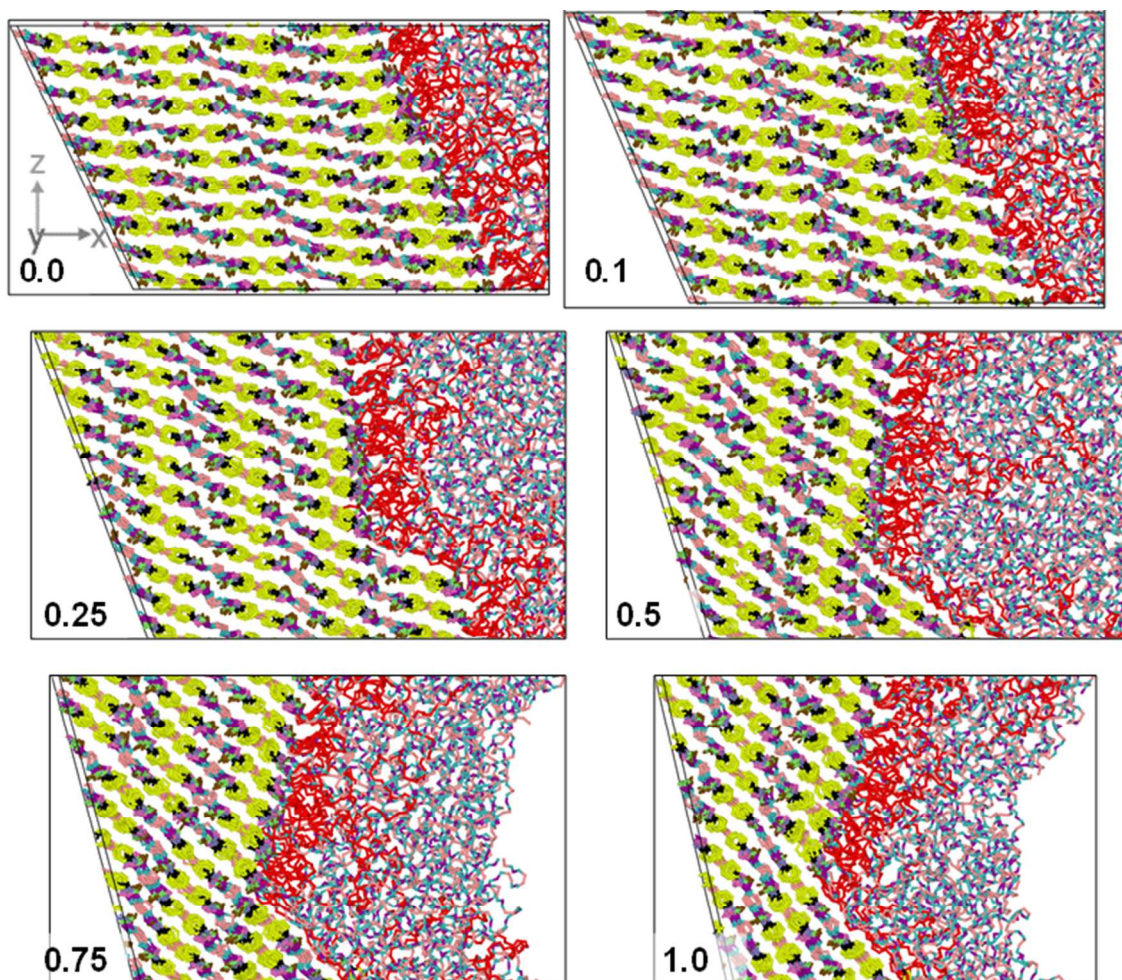


**Figure S5.** Evolution of structure for configuration #1 ("No bridges" sub-ensemble) under tensile deformation along z direction. Strain values are shown.

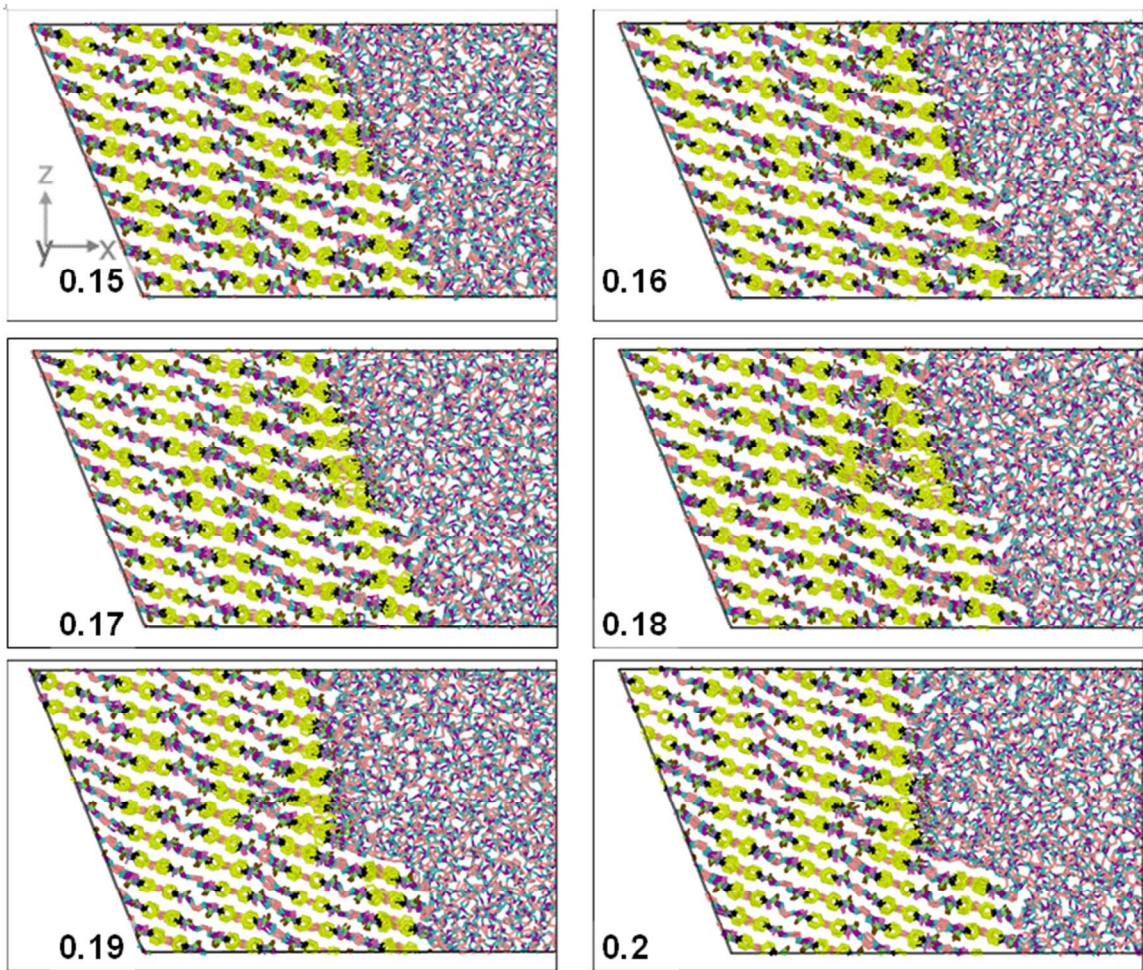


**Figure S6.** Initiation and completion of a block slip process for configuration #1 (system topological category: No bridges) under tensile deformation along z direction. Strain values are labeled.

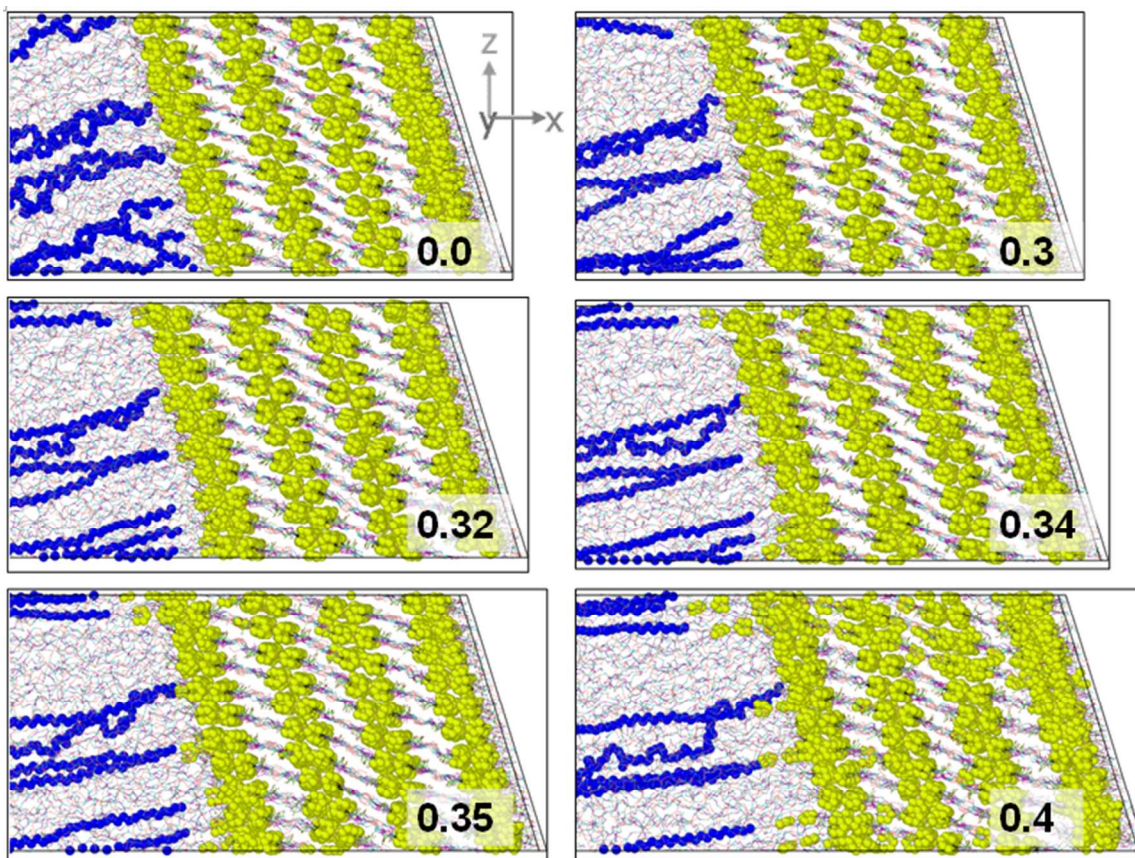


**Figure S7.** Pulling out processes for hard segments in configuration #6 (system topological category: With bridges) under tensile deformation along x direction. Strain values are labeled.

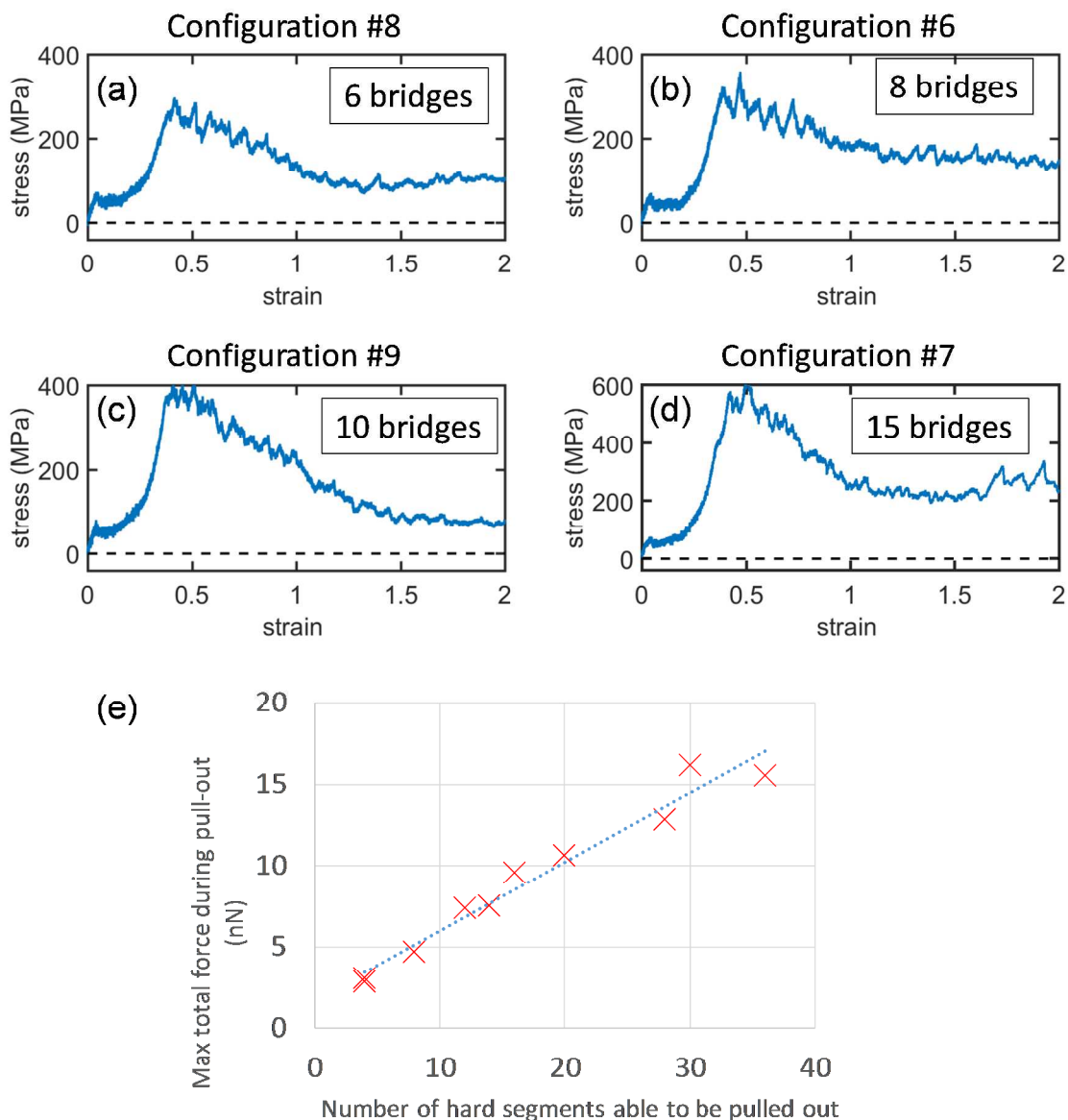


**Figure S8.** For cases containing bridges and not containing loop-loop bridge entanglements, the strength/maximum total force during pull-out is about linearly proportional to the number of bridges/number of hard segments able to be pulled out. The data in (e) contains all cases from “with bridges” sub-ensemble. The maximum total force is calculated from the strength times the cross-section area of the simulation box normal to the loading direction.

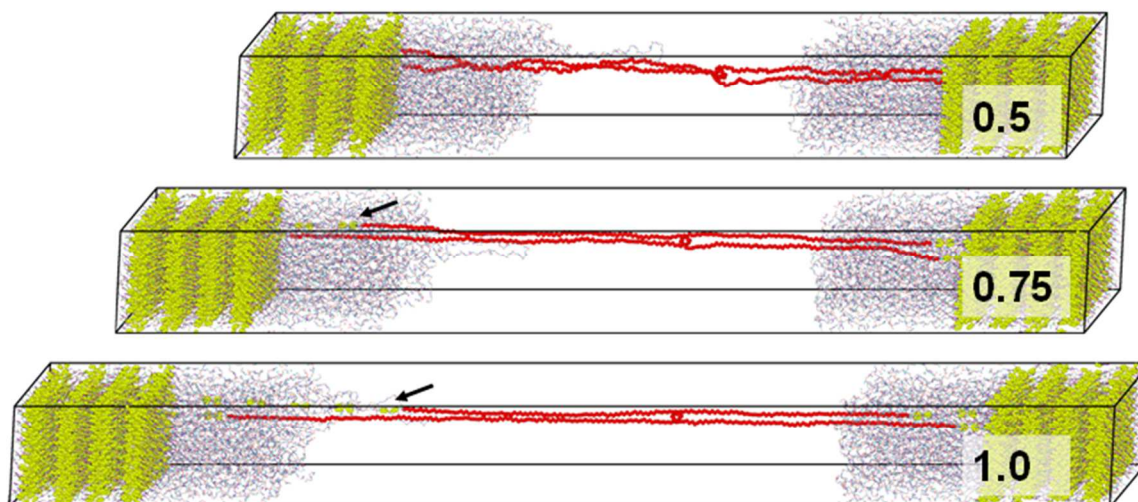


**Figure S9.** The “pulley effect” for a loop-loop bridging entanglement in configuration #11 (system topological category: With bridges). Strain values are labeled. A section of the hard segment pulled out of the hard domain is indicated by arrows; it moves faster than the hard segment being pulled out at the opposing interface. Eventually, only the first hard segment is completely pulled out.

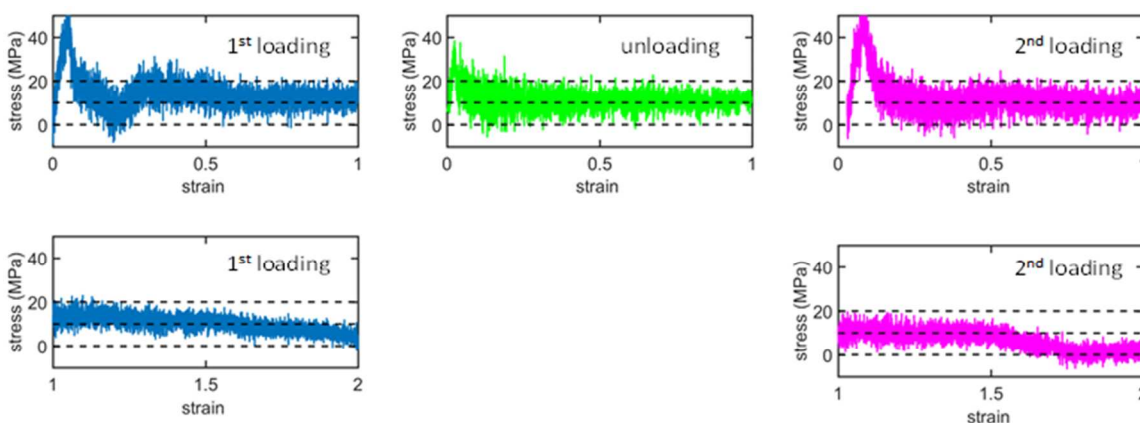


**Figure S10.** Softening of mechanical response for configuration #1 (system topological category: No bridges) during cyclic tensile straining along the x direction. Due to the unraveling of tails during the first loading, the stress during the second loading drops to zero (around 175% strain) faster than the stress during the first loading, caused by an earlier complete disentanglement.